

Eksploatacja i Niezawodnosc - Maintenance and Reliability

Volume 29 (2027), Issue 3

https://ein.org.pl

The Polish Maintenance Society

Data-driven predictive maintenance planning using bootstrap Kolmogorov–Smirnov validated three parameter Weibull model for maintenance decision support

Abir Mouldi[1,*]

[1] Department of Industrial Engineering, College of Engineering, King Khalid University, Saudi Arabia
* Corresponding Author: abir20052002@yahoo.fr

Received: 1 March 2026
Revised: 28 July 2026
Accepted: 21 September 2026
Online: 16 November 2026

This is an open access article under the CC BY 4.0 license

Abstract

Industrial plants often need to plan maintenance using routine logs and few repeated failures per component. This study proposes a transparent, uncertainty-aware predictive-maintenance workflow that converts maintenance records into time-between-failures data and fits a location-shifted three-parameter Weibull model via Benard median ranks and Weibull probability-plot regression. Parameter uncertainty is quantified with 95% bootstrap confidence intervals, and model adequacy is verified using a bootstrap-adjusted Kolmogorov–Smirnov test. Applied to two sewing-machine components (tension wire and hook), the validated models indicate decreasing hazard rates ($\beta<1$) and provide reliability metrics that guide inspection scheduling, preventive replacement windows and spare-parts provisioning. The results underline the value of reporting uncertainty and validating fit when decisions rely on sparse field data.

Keywords: *predictive maintenance, maintenance log data, three-parameter Weibull distribution, bootstrap resampling, Kolmogorov–Smirnov goodness-of-fit test*

Article citation:
Mouldi A, Data-driven predictive maintenance planning using bootstrap Kolmogorov–Smirnov validated three parameter Weibull model for maintenance decision support, Eksploatacja i Niezawodnosc – Maintenance and Reliability 2027: 29(3) http://doi.org/10.17531/ein/237615

Highlights

- Routine maintenance logs converted to time-between-failures datasets for key parts.
- Location-shifted three-parameter Weibull estimated by median ranks and probability plots.
- Bootstrap confidence bounds quantify Weibull-parameter uncertainty in small TBF samples.
- Bootstrap-adjusted Kolmogorov–Smirnov test validates Weibull model adequacy.
- Reliability and hazard guide inspection timing, replacement and spare-parts planning.

1. Introduction

In the new industrial context, companies face significant pressure from their customers. These customers are becoming increasingly demanding and also require high-quality products and services at lower costs, delivered quickly and on time [1]. To meet the demand for quality and quantity while respecting delivery times and costs, manufacturing companies must have well-maintained, reliable production machines [2,3]. Similarly, an unexpected shutdown is costly for a company [3].

Companies need to know the reliability of strategic machines, their lifespan, as well as the type of maintenance they should adopt, in order to meet their customers' needs [2,4]. Therefore, the maintenance engineer must implement a well-thought-out predictive and preventive maintenance plan so that breakdowns and production stoppages do not occur [4–6]. The majority of maintenance problems and systems lie in the random methods used to apply them and the failure to record all the details in order to be used as an important reference that builds a database that enables us to anticipate errors before they occur and arrange an organized and accurate maintenance system that organizes the operations and functions assigned to workers according to their different specializations [3,6]. The research focuses on the application of predictive maintenance using the Weibull distribution, which provides an accurate reading of the previous data, its analysis, and the extraction of

a specific function that applies to future data and predicts the upcoming failure in an approximate way [7,6]. Konwerski et al. integrated statistical and stochastic methods for estimating reliability and availability indicators from empirical failure data in technical systems [8]. Selech et al. analysed multi-year maintenance records to identify best-fit life distributions and to quantify reliability, maintainability and availability of complex vehicle subsystems [9].

Despite the rich literature on Weibull analysis and reliability modelling, a critical gap remains between academic methods and industrial practice when data are sparse. Most textbook treatments assume either large samples ($n > 30$) or the availability of censored test data from designed experiments. Most commercial reliability software outputs point estimates—a single MTBF, a single β, a single recommended replacement age—without quantifying the uncertainty that arises when n is as small as 7 or 16. Most academic papers introduce new estimators or complex models that require data conditions (sensors, covariates, complete failure histories) that routine maintenance logs do not provide.

In contrast, the typical maintenance engineer faces: (i) a spreadsheet or handwritten log with dates of failures and repairs; (ii) few repeat failures per component because replacements reset the clock; (iii) no controlled testing environment; (iv) no cost data for preventive vs. corrective actions; and (v) pressure to make a decision anyway. In this common but under-addressed setting, the engineer needs a workflow that is: data-driven (uses available failure records, however sparse); uncertainty-aware (does not pretend small samples give precise answers); transparent (the engineer can see why a model was chosen and whether it fits); and actionable (produces a maintenance recommendation, even if a range rather than a single date).

This gap—between what reliability theory assumes and what maintenance practice actually has—is the necessity that motivates the present study. We do not claim to invent new statistical estimators. Rather, we integrate existing methods (three-parameter Weibull, median-rank probability plotting, bootstrap resampling, KS goodness-of-fit) into a coherent workflow tailored for sparse field data, and we show how to translate the results into maintenance decisions without requiring cost data that industry often lacks.

There are several well-known estimation methods for fitting age data to a Weibull distribution: Ranked Regression (using the median ranks on the y values), Maximum Likelihood Estimation (MLE), and the Method of Moments [7,10]. The latter only considers the failure events, and so is not as useful [7]. Years ago, reliability engineers used specially printed log-log (probability plot) graph paper to manually plot the failure ages and fit a regression line by eye, before reading off the parameters that represented the Weibull distribution. The 'goodness of fit' of the regression line was seen by eye. Today specialized software is used to calculate the estimates [7,10]. Usually, people with an engineering background prefer the ranked regression method, because the probability chart allows the data and the fit to be visualized. It is easy to see whether the data suffers from mixed failure modes, or whether it is appropriate to use the location parameter from the visual line fit [7,10]. More advanced extensions also combine lifetime information with condition-monitoring variables using Weibull-based proportional hazards or mixture models to enhance failure prediction [11]. The consequent best-fit data is helpful for the maintenance engineers to make a strategic decision on identification of critical component, that is likely lead to machine failure [5,6,12]. In this present analysis a 3-parameter Weibull distribution has been considered to estimate the reliability of sub-systems [10,13].

Although predictive maintenance has received extensive attention in the context of Industry 4.0 [4], many plants still need to make reliability decisions using only routine maintenance records and small samples of time-between-failures data [14]. The ideal of big-data analytics contrasts sharply with the operational reality: maintenance logs may span years but contain few repeat failures for any specific component, production constraints prevent controlled reliability experiments, and heterogeneous operating conditions complicate data pooling. In such settings, a transparent and robust-to-small-samples statistical model that can be fitted from limited data and translated into maintenance actions is needed, especially when components exhibit early-life failures and a non-zero failure-free period. This paper therefore adopts a location-shifted three-parameter Weibull model rather than imposing the two-parameter constraint $\gamma = 0$. The choice is data-driven: in both components, the empirical Weibull plot under

the zero-shift assumption is distinctly curved, whereas introducing γ makes the transformed points approximately linear and gives γ a practical interpretation as a short failure-free interval after return to service. A two-parameter fit would force the support to start at t = 0 and would absorb this shift into β and η, potentially distorting early-life reliability and hazard estimates that are central to maintenance decisions. For estimation, median-rank probability-plot regression is used as the primary tool because it makes this curvature, the effect of ties, and possible mixed-failure behaviour directly visible to engineers [7,10]. The study does not claim that ranked regression is universally more efficient than maximum likelihood; rather, for sparse field data and a free location parameter, the graphical approach offers a transparent diagnostic basis, while bootstrap confidence intervals and a bootstrap-adjusted Kolmogorov-Smirnov test are used to quantify the uncertainty that would otherwise be hidden by a single point fit.

The innovation in this paper lies not in the 3P-Weibull itself, but in the integrated analytical-graphical workflow specifically designed for "sparse field data" (small samples). We provide a robust method for quantifying and propagating parameter uncertainty into actionable "decision windows" rather than single point-estimates, which is a critical gap in routine industrial maintenance.

2. Materials and methods

The estimation of equipment life is an important step in the decision-making process. Reliability analysis helps in this process to estimate the equipment life. One of the most utilized lifetime distributions for reliability is a Weibull distribution [15]. It is suitable distribution for factor estimation and shows the variety types of failure rate activities. On the basis of shape parameter, Weibull distribution is a versatile distribution that can take properties of other type of distributions.

This distribution can be found with two or three parameters; scale, shape and location parameters. There are a number of methods for estimating the values of these parameters; some are graphical and others are analytical. Graphical methods include Weibull probability plotting [12]. Especially, they incorporate the probability density function (PDF) plots.

While Maximum Likelihood Estimation (MLE) is statistically efficient in large samples, it often fails to converge or provides biased results for 3-parameter models with very small n (like our n=7 case), it can be unstable for small samples with a free location parameter γ. Ranked regression was chosen because it allows for visual diagnostic of the location shift and is more accessible to plant engineers for manual verification, it provides a visual diagnostic that engineers can interpret directly—curvature under γ=0, indicates need for γ, ties are visible, mixed failure modes detectable. We do not claim probability-plot regression is universally superior; we claim it is more robust and transparent for the specific sparse-data industrial setting.

Because industrial reliability modelling is often challenged by sparse field data and heterogeneous operating conditions, practical Weibull-based workflows that remain interpretable for engineers are still needed [14]. Moreover, fitted Weibull models can be translated into inspection and preventive replacement policies for maintenance planning under imperfect inspections [16]. Accordingly, the goal of this work is to model reliability from historical maintenance records for selected components at the case-study manufacturer and to derive actionable reliability and hazard functions to support maintenance timing decisions. Historical maintenance records were transformed into time-between-failures datasets for selected components, addressing the practical reality of sparse field data common in industrial settings. The empirical cumulative distribution was estimated using median ranks, with bootstrap confidence intervals employed to quantify parameter uncertainty inherent to small samples. Weibull model parameters were obtained through probability plotting and regression, introducing a location shift only when the zero-shift plot exhibited systematic curvature and the shifted plot became approximately linear. This rule links model choice to an observable diagnostic instead of treating the three-parameter form as automatic. Probability-plot regression was preferred as the primary estimation route because it preserves engineering interpretability: the analyst can directly assess the effect of γ, the handling of ties, and possible mixed-failure behaviour on the same plot [7,10]. Model adequacy was then evaluated using the Kolmogorov-Smirnov goodness-of-fit test with bootstrap-adjusted critical values to account for parameter estimation from limited data.

For double-blind review, company-identifying information

is withheld. The case study concerns a large multinational manufacturer operating a sewing-machine production environment.

2.1. Weibull model background

Due to its flexibility and interpretability, Weibull modelling is widely used to analyse life data for systems or subsystems and to quantify reliability and failure-rate behaviour [15,17]. Depending on the estimated parameters, the cumulative probability, failure rate, and probability density function (PDF) curves can take different shapes. Recent EiN research has also employed three-parameter Weibull distributions to model hard-failure processes within reliability assessment frameworks [18].

β is the Weibull shape parameter (slope). If β > 1, the hazard rate increases over time (often associated with wear-out). If β < 1, the hazard rate decreases (often associated with early-life or infant-mortality failures). If β = 1, the hazard rate is constant and the Weibull model reduces to the exponential distribution [15,17].

A typical "bathtub curve" (figure 1) depicts three regimes: early-life (infant mortality) phase with decreasing failure rate attributed to manufacturing defects, installation errors, or initial wear-in issues, useful-life phase with approximately constant failure rate representing random failures during normal operation, and wear-out phase with increasing failure rate due to aging, degradation, and material fatigue. Weibull models with different β values are commonly used to represent these regimes Understanding which phase a component occupies enables targeted maintenance strategies: burn-in testing for early life, preventive replacement for wear-out, and condition monitoring for useful life [15,17].

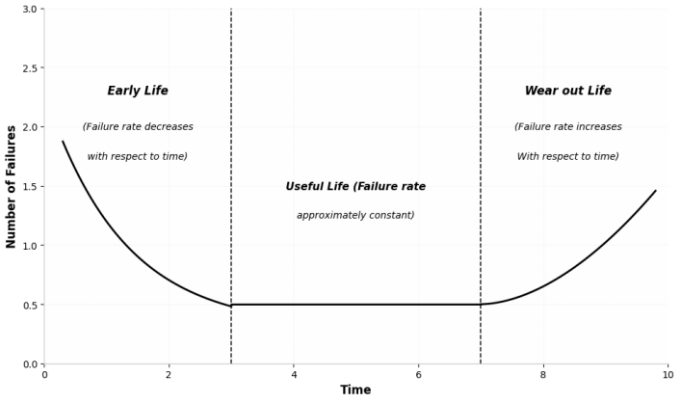


Figure 1. The bathtub curve illustrating the three characteristic phases of component failure behavior over time.

Weibull analysis can be performed with small samples, but the resulting parameter uncertainty can be substantial. For this reason, uncertainty bounds (e.g., bootstrap confidence intervals for β, η and MTBF) should be reported and used in maintenance decision-making when n is small [7,13,19].

Another advantage of Weibull analysis is the probability plot, which provides a simple visual diagnostic for engineers to assess fit quality, identify potential mixed failure modes, and interpret aging trends [12,19]. In the present study, this visual diagnostic is also the basis for choosing between the two- and three-parameter Weibull forms: persistent convexity or concavity under the zero-shift assumption is treated as evidence that a shifted life origin should be modelled, whereas approximate linearity would favour the simpler two-parameter representation.

2.2. Weibull distribution and linearisation

The cumulative distribution function (CDF) of the three-parameter Weibull distribution is:

$$F(t) = 1 - exp[-((t - \gamma) / \eta)\hat{}\beta], \qquad t \geq \gamma \quad (1)$$

where β > 0 is the dimensionless shape parameter, η > 0 is the scale parameter (days), and γ ≥ 0 is the location parameter (days) representing a failure-free period. When γ = 0, the model reduces to the two-parameter Weibull distribution.

The reliability function corresponding to Equation (1) is obtained as:

$$R(t) = 1 - F(t) = exp[-((t - \gamma) / \eta)\hat{}\beta] \quad (2)$$

To estimate the parameters graphically, the CDF is linearised by applying the double logarithm to both sides of Equation (1). Rearranging gives:

$$1 - F(t) = exp[-((t - \gamma) / \eta)\hat{}\beta] \quad (3)$$

Taking the natural logarithm twice yields:

$$ln[-ln(1 - F(t))] = \beta \cdot ln(t - \gamma) - \beta \cdot ln(\eta) \quad (4)$$

Equation (4) has the linear form $Y = \beta \cdot X + C$, where the transformed variables are defined as:

$$Y = ln[-ln(1 - F(t))] \quad (5)$$

$$X = ln(t - \gamma) \quad (6)$$

and the intercept term is:

$$C = -\beta \cdot ln(\eta) \quad (7)$$

Thus, the shape parameter β is the slope of the regression line, and the scale parameter η is recovered from the intercept

via:

$$\eta = exp(-C / \beta) \quad (8)$$

The Weibull probability plot displays Y against X (or against ln(t) when γ = 0).

Case 1: γ = 0 (two-parameter Weibull). When the plotted points (ln(t), Y) are approximately linear with γ = 0, the two-parameter model is adequate. The characteristic life η is read at the intersection of the fitted line with the 63.2% unreliability level (i.e., Y = 0), since $F(\eta) = 1 - e^{-1} \approx 0.632$. Formally, setting Y = 0 in Equation (3) with γ = 0 gives:

$$0 = \beta \cdot ln(\eta) - \beta \cdot ln(\eta) \quad \rightarrow \quad ln(t) = ln(\eta) \quad (9)$$

which confirms that η is the time at which 63.2% of components have failed [15,21].

Case 2: γ ≠ 0 (three-parameter Weibull). When the (ln(t), Y) plot under γ = 0 exhibits systematic curvature — concave upward or concave downward — a non-zero location parameter is indicated. Figure 2 illustrates both curvature types. The three-point estimation method proceeds as follows:

(a) Select three points on the empirical CDF curve with equally spaced ordinates F_1, F_2, F_3 on the linear probability scale and read the corresponding abscissae t_1, t_2, t_3 on the linear TBF axis (not on the ln–ln Weibull scale).

(b) The three points on the curve have coordinates $M_1(t_1, F_1)$, $M_2(t_2, F_2)$, and $M_3(t_3, F_3)$. Because F_1, F_2, and F_3 are equally spaced on the ordinate axis, the condition of collinearity after shifting by γ yields:

$$(t_2 - t_1) / (t_3 - t_1) = [(t_2 - \gamma) - (t_1 - \gamma)] / [(t_3 - \gamma) - (t_1 - \gamma)] \quad (10)$$

(c) Solving Equation (8) for γ gives the explicit estimator:

$$\gamma = t_2 - [(t_3 - t_2)(t_2 - t_1)] / [(t_3 - t_2) - (t_2 - t_1)] \quad (11)$$

(d) All observed failure times are then shifted: $t_i* = t_i - \gamma$.

(e) The remaining parameters β and η are obtained from the linear regression of Y on $X = ln(t_i*)$, as described in Case 1.

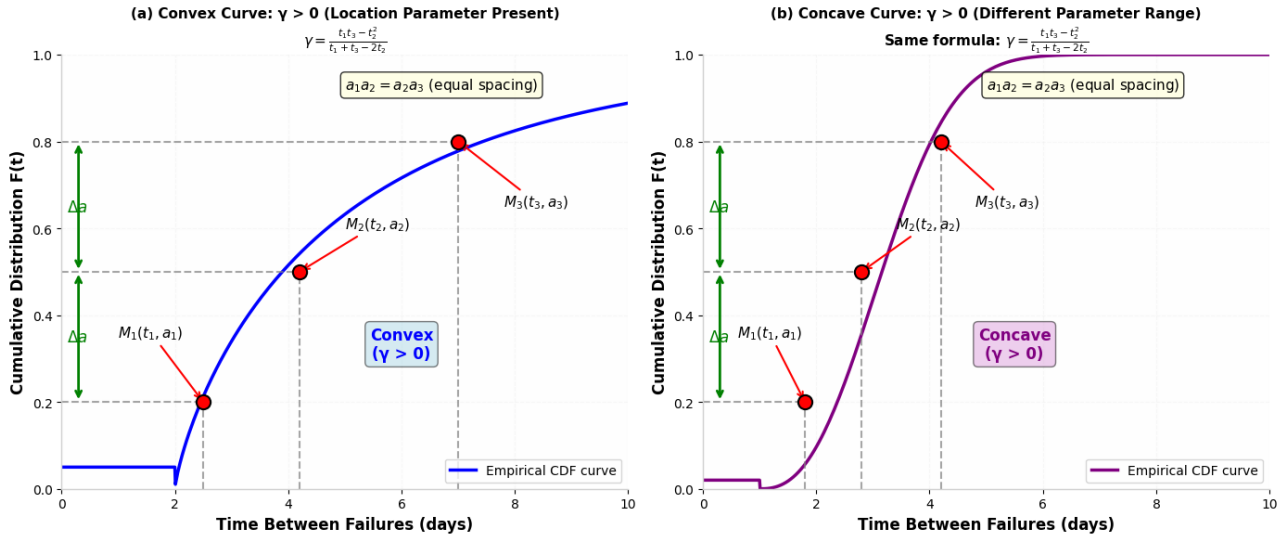


Figure 2. Graphical estimation of the three-parameter Weibull location parameter γ using the three-point method on empirical CDF curves plotted against time between failures; (a) Convex curve case (b) Concave curve case.

The mean time between failures (MTBF) for the three-parameter Weibull distribution is obtained from the expected value of the reliability function. In terms of the Euler gamma function of the second kind, Γ(·), the MTBF is:

$$MTBF = \gamma + \eta \cdot \Gamma(1 + 1/\beta) \quad (12)$$

The variance of the time to failure is expressed as:

$$\sigma^2 = \eta^2 \cdot [\Gamma(1 + 2/\beta) - (\Gamma(1 + 1/\beta))^2] \quad (13)$$

and the standard deviation is the square root of Equation (13).

2.3. Empirical CDF estimation

We have a number of experimental and real-world data for our reliability studies. These data represent a sample n of the population that we want to apprehend.

For complete (uncensored) samples, the empirical unreliability was estimated using median-rank plotting positions. Using Benard's approximation, the i-th ordered failure time is assigned [20,21]:

$$F_i = \frac{i-0.3}{n+0.4} \quad i = 1, \ldots\ldots, n \quad (14)$$

where n is the sample size. These plotting positions were used to construct the empirical CDF and to build the Weibull probability plot [13,14]. The procedure for ranking complete data is as follows:

1. List the time to failure data from small to large.

2. Use Benard's formula to assign median ranks to each failure.

3. Estimate the γ, β and η.

2.4. Goodness-of-fit testing

The Kolmogorov-Smirnov (KS) test is a goodness-of-fit test used to accept or reject the hypothesis that the data follow a specified distribution at a chosen significance level [23,24]. The test compares the hypothesized CDF (here, the fitted Weibull CDF) with an empirical CDF derived from the data. For complete data, the empirical CDF was constructed using median-rank plotting positions, e.g., [20,22]. The maximum absolute difference between the two CDFs defines the KS statistic D [23,24]. Given the significance level alpha and the sample size n, a critical value Dcrit is obtained; the null hypothesis is accepted when D < Dcrit [23,24]. Because the Weibull parameters are estimated from the same sample, classical KS critical values should be interpreted as approximate. To address this limitation, a parametric bootstrap was also used to obtain a bootstrap p-value for the observed KS statistic by simulating samples from the fitted Weibull model, re-estimating parameters, and recomputing the KS statistic [7,13].

$$Dmax = \max_i \left|F_{emp}(t_i) - F_{model}(t_i)\right| \quad (15)$$

For the Kolmogorov-Smirnov test at significance level $\alpha = 0.05$, the critical value is approximated by:

$$D_{crit} = \frac{K_\alpha}{\sqrt{n}} \quad (16)$$

Where n is the sample size and K_α is the Kolmogorov-Smirnov critical value constant.

2.5. Small-sample reliability methodology

Industrial reliability modeling is frequently constrained by sparse field data resulting from the practical realities of maintenance operations: components are replaced upon failure (preventing multiple observations), production pressures limit experimental testing, and record-keeping may be incomplete [14]. Rather than treating small sample sizes as a limitation to overcome, this work adopts a small-sample methodology that explicitly quantifies uncertainty through bootstrap resampling.

For the tension wire (n = 7) and hook (n = 16) datasets, uncertainty was quantified with a parametric bootstrap. Specifically, 1,000 synthetic samples of size n were generated from the fitted three-parameter Weibull model for each component; the Weibull parameters, MTBF and KS statistic were then re-estimated for every replicate. This point is important for interpretation: the procedure does not repeatedly resample only the seven observed tension-wire values, so the objection that the number of distinct resamples is severely limited applies to the nonparametric bootstrap, not to the model-based procedure used here. In the present setting, the role of B = 1,000 is to control Monte Carlo error in the approximation of the fitted model's sampling distribution, not to create additional information beyond the observed failures. For a bootstrap p-value , the simulation error is approximately

$$\sqrt{p(1-p)/B} \quad (17)$$

with $B = 1{,}000$ this is about 0.016 at $p = 0.45$ for the tension wire and about 0.010 at $p = 0.12$ for the hook, so the bootstrap accept/reject conclusions are numerically stable at the 5% level. Likewise, for 95% percentile intervals, $B = 1{,}000$ yields tail estimates based on approximately the $25th$ and $975th$ ordered replicates, which is adequate for the approximate uncertainty bounds targeted here. Increasing B would smooth the interval endpoints slightly, but it would not reduce the dominant uncertainty arising from the small original sample [7,13].

Because component-specific cost data for downtime, inspection, preventive replacement and corrective replacement were not available from the routine maintenance records, the conversion from reliability results to maintenance timing was based on a reliability-target rule rather than an economic optimisation model.

Justification of the reliability threshold. The choice of R(t) = 0.5 as the preventive replacement threshold is motivated by three considerations. First, R(t) = 0.5 corresponds to the median life $t_{0.5}$, which is a distribution-free measure of central tendency. Unlike the mean (MTBF), the median is robust to the right-skewness typical of Weibull distributions with β < 1. Second, in the absence of component-specific cost data — preventive

replacement cost Cp and corrective (failure-based) replacement cost Cc — the median provides a neutral planning benchmark that does not implicitly assume any particular cost ratio. Third, when cost data become available, the optimal reliability threshold for age-based replacement under the long-run average cost criterion can be expressed as $R(t*) = Cp / (Cp + Cc)$ within the classical age-replacement framework [26]. Adopting R(t) = 0.5 is therefore equivalent to assuming Cp ≈ Cc as a reasonable starting point in the absence of empirical cost data.

The point preventive-replacement age $t*$ was therefore defined by $R(t*) = R*$; for the three-parameter Weibull model this gives

$$t* = \gamma + \eta[-ln(R*)]\hat{}(1/\beta) \quad (18)$$

To propagate parameter uncertainty into maintenance decisions, a practical intervention window $[tL, tU]$ was derived from the 95% bootstrap reliability band: tL is the first age at which the lower confidence bound of $R(t)$ falls to $R*$, and tU is the first age at which the upper confidence bound falls to $R*$. Thus, the lower limit corresponds to a conservative, risk-averse intervention age, whereas the upper limit corresponds to the latest age that remains compatible with the fitted model without additional condition information.

To assess the sensitivity of maintenance timing to the chosen threshold, the preventive replacement age was recomputed for R_target ∈ {0.5, 0.7, 0.8}. These results are reported and discussed in Section 4.1.

2.6. Comparison with existing reliability engineering procedures

The proposed workflow improves upon common alternatives in four key respects. First, unlike fixed-interval replacement (e.g., "replace every 30 days"), it is data-driven, using the component's actual failure history rather than heuristic schedules. Second, unlike point-estimate reliability (e.g., "MTBF = 38.5 days"), it quantifies uncertainty via bootstrap confidence intervals—for the tension wire (n=7), the 95% MTBF interval is 10–120 days, a range that fundamentally changes maintenance planning. Third, unlike standard Kolmogorov–Smirnov testing, it uses bootstrap-adjusted p-values that correctly account for parameter estimation from the same data. Fourth, unlike cost-optimisation models, it does not require unavailable cost data; instead, it produces reliability-target decision windows (e.g., "replace between 10–35 days") that give engineers a risk-based range rather than a false-precision point estimate.

3. Results

Failure and repair records for the studied sewing machines were extracted from the company's routine maintenance documentation (daily handwritten reports and the computerized maintenance database) for the 2024–2025 observation period. For each component (tension wire and hook), the recorded failure timestamps were converted into time-between-failures (TBF) observations measured in days. In this work, TBF is used as the component time-to-failure (age) for each renewal cycle: time zero is defined at the return-to-service moment after corrective maintenance (replacement/repair), and the interval ends at the next recorded failure of the same component. Tables 1–2 list the observed TBF values; repeated durations are reported as frequencies $\sum n_j$ for compactness, but all subsequent analyses (median-rank empirical CDF, Weibull probability plotting, KS goodness-of-fit testing, and bootstrap uncertainty quantification) use the full set of failure intervals with n =$\sum_i \sum n_j$ observations (tension wire: n = 7; hook: n = 16), retaining ties as repeated events.

Table 1. Historical data of the tension wire.

$Order(i)$	$TBF(i)$	$\sum n_j$
1	2	1
2	4	2
3	10	1
4	15	1
5	31	1
6	114	1

Table 2. Historical data of the hook.

$Order(i)$	$TBF(i)$	$\sum n_j$
1	2	2
2	3	1
3	4	1
4	5	2
5	7	1
6	8	1
7	10	1
8	15	1
9	16	2
10	17	1
11	21	1
12	25	1
13	47	1

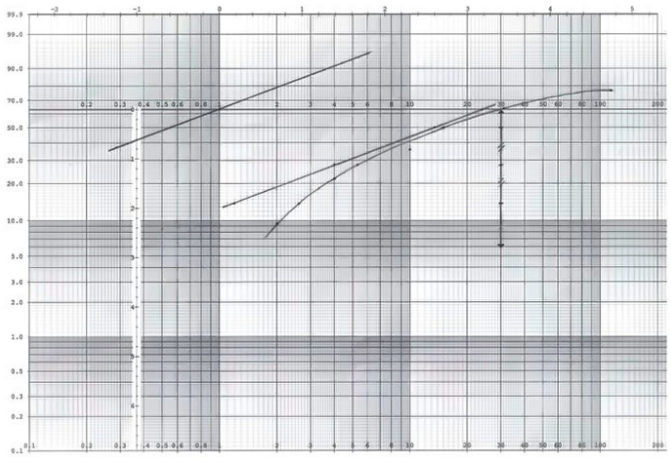
The calculation of the estimated theoretical cumulative distribution function is determined by the formula of median ranks (17) as shown in tables 3 and 4 for tension wire and the hook.

Table 3. Empirical cumulative distribution function of the tension wire.

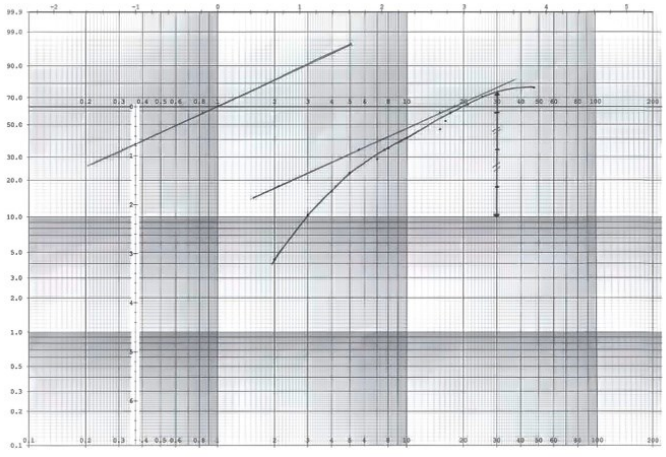
$Order(i)$	$TBF(i)$	$Femp(i)\%$
1	2	9.45
2	4	22.97
3	4	36.49
4	10	50
5	15	63.51
6	31	77.03
7	114	90.54

Table 4. Empirical cumulative distribution function of the hook.

$Order(i)$	$TBF(i)$	$Femp(i)\%$
1	2	4.27
2	2	10.37
3	3	16.46
4	4	22.56
5	5	28.66
6	5	34.76
7	7	40.85
8	8	46.95
9	10	53.05
10	15	59.15
11	16	65.24
12	16	71.34
13	17	77.44
14	21	83.54
15	25	89.63
16	47	95.73



(a)



(b)

Figure 3. Weibull plot (a) of the tension wire and (b) of the hook.

3.1. Weibull probability plotting

A Weibull Probability plotting paper is constructed by logarithmic cumulative density function (CDF) or unreliability function of the distribution (y-axis) as a function of a logarithmic TBF x-axis. Figures 3 shows the curve plotting of CDF of respectively the tension wire and the hook using failure data. The slope of the fitted line corresponds to the shape parameter β, the characteristic life η is determined at the intersection of the fitted line with the 63.2% unreliability level.

The representation of the function $(TBF(i),\ Femp(i))$ gives for the two cases: the tension wire and the hook a convex curve which implies that γ is different from zero, requiring three-point estimation to achieve linearity. Table 5 resumes the computed values of the three Weibull parameters, the reliability expressions and the reliability drivers MTBF and the standard deviation.

Table 5. Computed values of reliability parameters.

Component	γ (days)	β	η (days)	R(t)	MTBF (days)	σ (days)
Tension Wire	1.4	0.6	24	$e^{-(\frac{t-1.4}{24})^{0.6}}$	38.5	63.6
Hook	2.1	0.8	18	$e^{-(\frac{t-2.1}{18})^{0.8}}$	22.49	25.74

3.2. Kolmogorov-Smirnov goodness-of-fit results

The tables 6 and 7 show the summaries and comparative tables corresponding to respectively the tension wire and the hook. The tables compare the values of the estimated cumulative density functions found through modeling and the empirical values of cumulative density function calculated using median rank method.

$\boldsymbol{D_{max}} = |Femp(i) - Fmodel(i)|$ measures the largest deviation between the distributions.

Table 6. Difference between hypothesized and empirical CDF for the tension wire.

$Order(i)$	$TBF(i)$	$Femp(i)$	$Fmodel(i)$	$\lvert Femp(i) - Fmodel(i)\rvert\%$
1	2	9.46	10.36	0.90
2	4	22.97	23.17	0.19
3	4	36.49	23.17	13.32
4	10	50.00	41.74	8.26
5	15	63.51	50.89	12.62
6	31	77.03	67.83	9.20
7	114	90.54	92.02	1.48

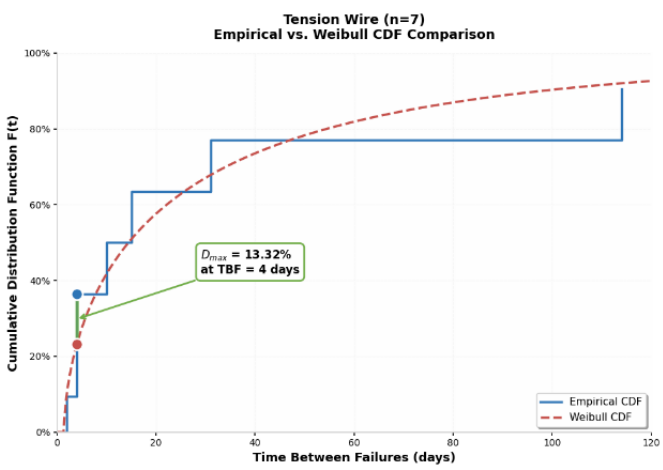
According to the table 6 we find $D_{7;0.05} = 51.4\%$ and $D_{max} = 13.32\%$ for the tension wire and the table 7 shows that $D_{16;0.05} = 34\ \%$ and $D_{max} = 19.77\ \%$ for the hook.

Figures 4 and 5 reflect the median-rank treatment in which repeated TBF values are retained as separate observations. For

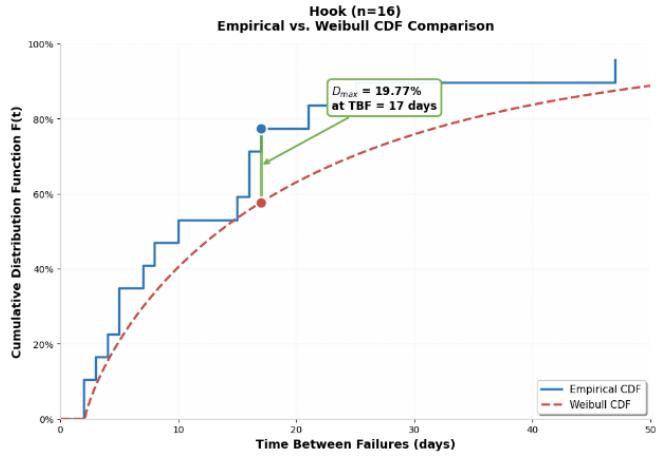
the tension wire, the maximum difference between the empirical and fitted Weibull CDF is $Dmax$= 13.32% at TBF = 4 days. For the hook, $Dmax$ = 19.77% at TBF = 17 days. The largest departures therefore occur in the early-to-middle part of the failure history, not at the final observation.

Table 7. Difference between hypothesized and empirical CDF for the hook.

$Order(i)$	$TBF(i)$	$Femp(i)$	$Fmodel(i)$	$\lvert Femp(i) - Fmodel(i)\rvert$%
1	2	4.27	0	4.27
2	2	10.37	0	10.37
3	3	16.46	8.70	7.76
4	4	22.56	15.25	7.31
5	5	28.66	20.71	7.94
6	5	34.76	20.71	14.04
7	7	40.85	29.75	11.10
8	8	46.95	33.61	13.34
9	10	53.05	40.40	12.65
10	15	59.15	53.52	5.63
11	16	65.24	55.66	9.59
12	16	71.34	55.66	15.69
13	17	77.44	57.67	19.77
14	21	83.54	64.65	18.89
15	25	89.63	70.25	19.38
16	47	95.73	87.48	8.25



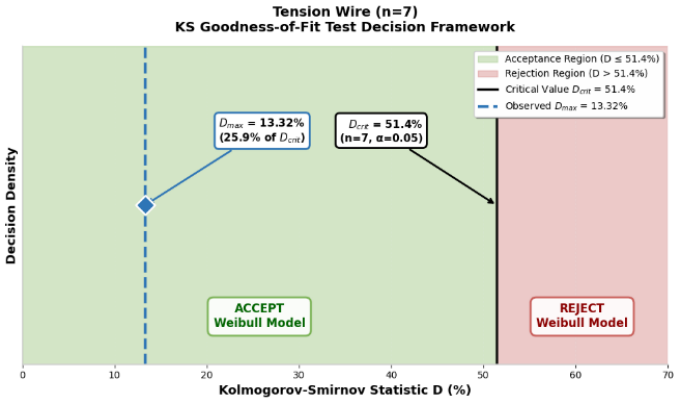
(a)



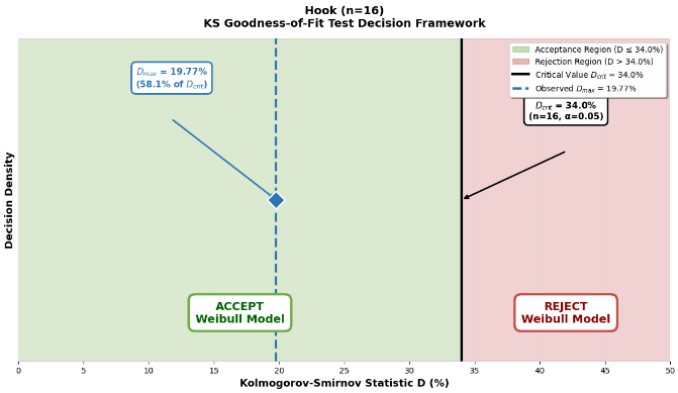
(b)

Figure 4. Difference between hypothesized and empirical CDF for (a) the tension wire and (b) for the hook.

The empirical and theoretical CDFs show acceptable overall agreement for both components. The fit is visibly closer for the tension wire, whereas the hook displays a larger local deviation around 16-17 days, indicating that the three-parameter Weibull model is useful but less exact for the hook in that region.



(a)



(b)

Figure 5. Decision visualization showing Dmax for (a) the tension wire and (b) for the hook.

Figure 5 visualizes the classical KS decision framework. For the tension wire, $Dmax$ = 13.32% remains well below the critical value D_{crit} = 51.4% for n=7 at α = 0.05, so the model is comfortably accepted. For the hook, $Dmax$ = 19.77% is also below D_{crit} = 34.0% for n=16, so the Weibull model is again not rejected, although the margin is smaller than for the tension wire. The bootstrap results in Table 8 lead to the same practical conclusion: p = 0.45 for the tension wire and p = 0.12 for the hook do not indicate rejection at the 5% level. Overall, the analysis supports using the fitted Weibull models for maintenance decision support, while acknowledging stronger local mismatch for the hook.

3.3. Model comparison and selection

To verify that the three-parameter Weibull distribution is the

most appropriate model for the observed failure data, a comparison was conducted against two alternative lifetime distributions: the two-parameter Weibull ($\gamma = 0$) and the lognormal distribution. Parameters for each candidate model were estimated by maximum likelihood, and model fit was assessed using the log-likelihood (LL), the Akaike Information Criterion (AIC = 2k − 2LL), and the Bayesian Information Criterion (BIC = $k \cdot \ln(n) - 2LL$), where k is the number of free parameters and n is the sample size. Lower AIC and BIC values indicate a better balance between goodness-of-fit and model complexity.

Table 8 summarises the comparison. For both components, the three-parameter Weibull achieves the lowest AIC and BIC, confirming that including the location parameter γ improves model adequacy relative to the simpler two-parameter form. The lognormal distribution performs worst for both datasets.

Table 8. Model comparison using maximum log-likelihood, AIC, and BIC.

Component	*Model*	*k*	*LL*	*AIC*	*BIC*
Tension wire ($n = 7$)	3P-Weibull	3	−28.19	62.37	62.21
	2P-Weibull	2	−29.71	63.42	63.31
	Lognormal	2	−30.28	64.55	64.44
Hook ($n = 16$)	3P-Weibull	3	−61.73	129.46	131.77
	2P-Weibull	2	−63.90	131.79	133.33
	Lognormal	2	−64.56	133.12	134.66

The ΔAIC values between the 3P-Weibull and the next-best model are 1.05 for the tension wire and 2.33 for the hook. Following Burnham and Anderson (2002), $\Delta AIC < 2$ indicates substantial support for both models, whereas ΔAIC between 2 and 4 indicates considerably less support for the alternative [25]. The comparison therefore supports the choice of the three-parameter Weibull for both components, with stronger justification for the hook dataset. It should be noted that for very small samples such as the tension wire (n = 7), AIC and BIC comparisons should be interpreted cautiously, as the penalty terms are based on asymptotic theory. Nevertheless, the consistency of the result across both criteria and both components, together with the visible curvature in the probability plot under $\gamma = 0$, provides converging evidence for the three-parameter specification.

4. Discussion

4.1. Analysis and maintenance implications

The median-rank treatment does not change the main physical interpretation of the Weibull parameters, but it sharpens their meaning. For the tension wire, β = 0.6 indicates a pronounced decreasing failure rate typical of early-life or installation-related failures. For the hook, β = 0.8 also indicates a decreasing hazard, but the effect is milder and the hazard approaches a more stable useful-life regime sooner.

The scale parameter η shows that the hook has a shorter characteristic life than the tension wire (18 vs. 24 days), so it reaches comparable reliability loss sooner under similar operating conditions. At the same time, the tension wire has the higher MTBF (38.5 days vs. 22.49 days), which reflects a longer right tail rather than uniformly better reliability across all ages.

The location parameter γ suggests a short failure-free period for both components: about 1.4 days for the tension wire and 2.1 days for the hook. This means the hook appears slightly more resistant during the first few days after return to service, but once failures begin, its characteristic life is shorter and its reliability declines faster overall.

The tension-wire results also reveal much larger dispersion in failure behaviour. Its standard deviation (63.6 days) is far higher than that of the hook (25.74 days), which means some tension wires fail very early while others survive much longer. This wide spread is consistent with the broad bootstrap confidence intervals and makes a single fixed replacement time less precise for the tension wire.

For the hook, the lower variability and narrower confidence intervals make its reliability pattern easier to interpret operationally. However, the KS comparison shows a larger local mismatch between the empirical and fitted Weibull CDF around TBF = 17 days, so the hook model should be used as a practical approximation rather than as an exact description of every quantile.

From a maintenance perspective, both components require attention soon after replacement because both fitted β values are below 1. For the tension wire, the stronger infant-mortality signature supports burn-in, installation-quality checks, and early post-replacement inspections. Because uncertainty is wide, conservative spare-parts buffering and condition-based follow-up are preferable to relying on a narrow fixed preventive interval.

For the hook, the key issue is not severe early-life scatter but a shorter characteristic life combined with moderate uncertainty. The maintenance recommendation is not heuristic: it is obtained

from the reliability-target rule R(t) = 0.5 defined in Section 2.5. The point estimate reaches this threshold at about 13.5 days, while the lower and upper 95% bootstrap reliability bounds cross the same threshold at about 12 and 25 days, respectively. Hence, 12-25 days is interpreted as the uncertainty-aware preventive replacement window: the lower end is appropriate for a conservative policy that prioritises downtime avoidance, whereas the upper end represents the latest age supportable without further condition evidence.

In contrast, the tension wire reaches R(t) = 0.5 at about 14.4 days, but the same rule produces a much wider 10-35 day window because parameter uncertainty is much larger. This range should therefore be interpreted as a decision zone rather than a single preferred interval: early intervention near 10-15 days is justified when downtime risk is costly, while operation toward the upper part of the window should be accompanied by closer inspection or condition checks. Overall, both components exhibit decreasing hazard rates, but the tension wire is dominated by higher uncertainty whereas the hook is dominated by shorter effective life.

Sensitivity to the reliability threshold. Table 9 reports the preventive replacement ages derived under three alternative reliability thresholds: $R(t) = 0.5$ (median, baseline), $R(t) = 0.7$, and $R(t) = 0.8$ (progressively more conservative). For each threshold, the point estimate and the 95% bootstrap confidence interval are provided.

Table 9. Sensitivity of preventive replacement age to the reliability threshold.

Component	Threshold R(t)	Point estimate (days)	95% bootstrap window (days)
Tension wire	0.5	14.4	10 – 35
	0.7	9.8	6 – 25
	0.8	7.2	4 – 19
Hook	0.5	13.5	12 – 25
	0.7	9.2	8 – 18
	0.8	6.8	5 – 14

The results confirm that the replacement window shifts predictably toward shorter ages as the reliability requirement becomes more stringent. Importantly, the width of the uncertainty window also narrows at higher thresholds because the reliability curve is steeper in the early-failure region for distributions with β < 1. This provides an additional practical insight: when operating under a conservative threshold, the maintenance schedule is not only earlier but also better identified from the available data.

These results position R(t) = 0.5 as a plausible default for non-critical components where preventive and corrective costs are roughly balanced. For safety-critical or high-downtime-cost assets, the more conservative thresholds R(t) = 0.7 or R(t) = 0.8 are recommended, and the corresponding windows in Table 9 can be adopted directly.

4.2. Limitations and uncertainty

The tension-wire dataset contains only seven observed failure intervals, so uncertainty in the fitted Weibull parameters and derived maintenance thresholds are substantial. To quantify this uncertainty, Table 10 reports bootstrap-based 95% confidence intervals for the Weibull shape (beta) and scale (eta) parameters (conditional on the estimated location shift gamma) and for the implied MTBF, together with the bootstrap KS p-value for each component. Because the location parameter gamma is particularly sensitive when n is small, the results should be interpreted as decision support and updated as additional failure data become available. In addition, the KS decision is supplemented with bootstrap p-values (Table 10) to reduce the common concern that classical KS critical values are optimistic when parameters are estimated from the same data [7,13,24].

Table 10. Bootstrap-based 95% confidence intervals (conditional on gamma) and bootstrap KS p-values.

Component	Sample size n	β 95% CI	η 95% CI (days)	MTBF 95% CI (days)	Bootstrap KS p-value
Tension Wire	7	[0.350, 1.45]	[6.00, 85.00]	[10.00, 120.00]	0.45
Hook	16	[0.550, 1.250]	[9.50, 35.00]	[13.00, 40.00]	0.12

The bootstrap confidence intervals in Table 10 confirm that uncertainty is much larger for the tension wire than for the hook. For the tension wire, β spans 0.35-1.45 and η spans 6-85 days, showing that both the hazard pattern and the maintenance timing remain only loosely identified. For the hook, the intervals β = 0.55-1.25 and η = 9.5-35 days are noticeably narrower, which supports more stable maintenance planning.

The bootstrap-adjusted KS results are also informative. To avoid confusion between the observed KS statistic Dmax and a single rounded bootstrap cutoff, Table 10 reports the bootstrap p-value rather than a separate bootstrap critical bound. For the tension wire, the bootstrap p-value of 0.45 indicates that the empirical CDF is fully compatible with the fitted Weibull model. For the hook, the bootstrap p-value of 0.12 does not indicate

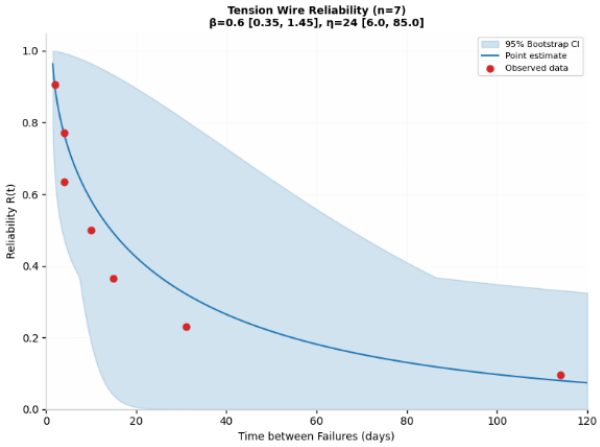
rejection, but it is closer to the decision boundary and consistent with the larger local deviation seen in the empirical-versus-theoretical CDF comparison. Thus, model adequacy is acceptable for both components, yet stronger confidence is warranted for the tension wire fit than for the hook fit.

With n = 7, the bootstrap results for the tension wire should therefore be read as conditional on the assumed three-parameter Weibull family. The bootstrap cannot recover information that is not present in the data; instead, it propagates the uncertainty implied by the fitted model and makes that uncertainty explicit. This is why the tension-wire intervals remain wide even after 1,000 replicates and why the resulting maintenance window is presented as a risk-based decision range rather than as a precise optimal age. Alternative small-sample approaches, including Bayesian or fiducial methods, could be explored in future work, but they would require additional prior or structural assumptions that were not available from the maintenance records.

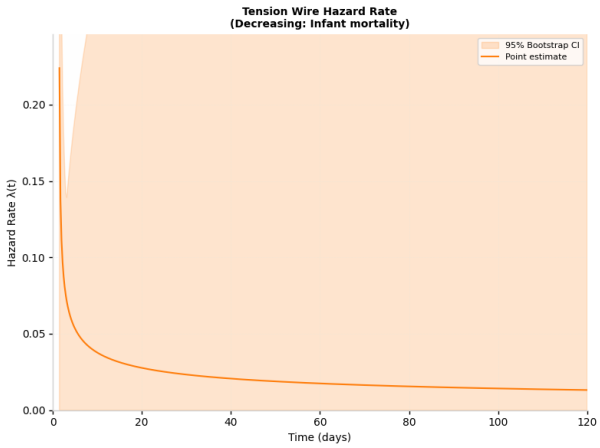
This study therefore treats small-sample industrial reliability estimation as an uncertainty-quantification problem rather than as a search for deceptively precise point values. The reported replacement windows are reliability-based planning thresholds, not economically optimal ages, because component-specific cost data for preventive and corrective actions were not available from the maintenance records. The wide tension-wire intervals are not a methodological failure; they are an honest reflection of the information content available in sparse field data. Maintenance engineers can use the lower MTBF or reliability bounds for conservative planning of inspections and spare parts, while revising policies as the failure history grows.

The location parameter γ remains especially sensitive with small samples. Its estimate of 1.4 days for the tension wire and 2.1 days for the hook should be interpreted as approximate minimum-life indicators rather than hard thresholds. Continued maintenance logging will allow the bootstrap procedure to be repeated, the intervals to narrow, and the maintenance policy to move from broad risk-based windows toward more precise scheduling.

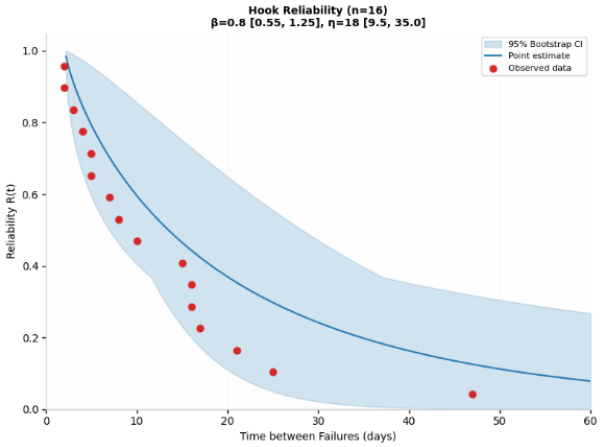
Figures 6 and 7 show how the Weibull analysis and bootstrap uncertainty propagate into maintenance decisions. Figure 6 indicates that the tension wire (n=7) carries substantially wider uncertainty bands than the hook (n=16): its bootstrap intervals are β in [0.35, 1.45] and η in [6, 85] days, whereas the hook is confined to β in [0.55, 1.25] and η in [9.5, 35] days. Both point estimates correspond to decreasing hazard rates, but the tension wire shows stronger infant-mortality behaviour and much wider dispersion in R(t), while the hook shows a milder decrease in hazard and more concentrated reliability trajectories. Figure 7 applies the decision rule defined in Section 2.5: the point preventive-replacement age is the time at which the fitted reliability curve reaches R(t) = 0.5, and the practical decision window is bounded by the ages at which the lower and upper 95% bootstrap reliability curves cross the same threshold. Under this rule, the point times are about 14.4 days for the tension wire and 13.5 days for the hook. Because uncertainty differs markedly, the resulting decision windows do too: about 10-35 days for the tension wire and 12-25 days for the hook. Thus, the tension-wire recommendation is broad because the data are sparse, whereas the hook supports a narrower scheduled replacement window.



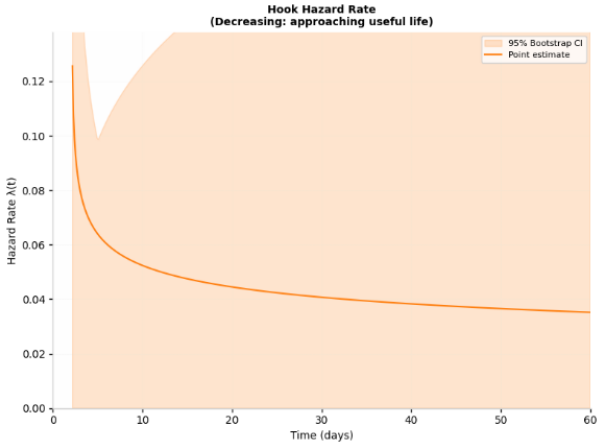
(a)



(b)

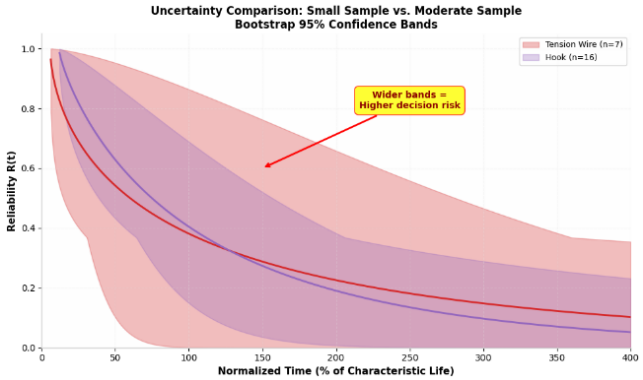


(c)

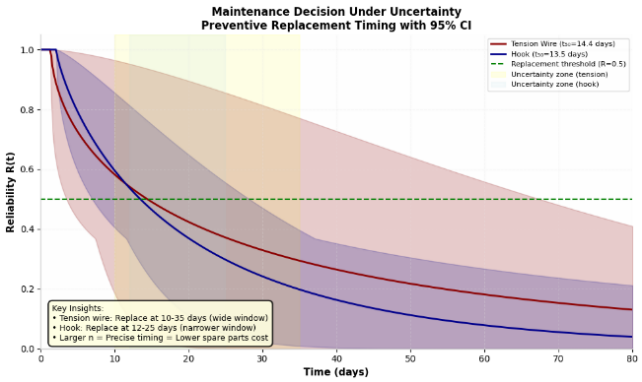


(d)

Figure 6. Bootstrap uncertainty quantification for Weibull reliability and hazard functions. (a) Tension wire reliability (n=7) with wide 95% confidence bounds reflecting parameter uncertainty. (b) Tension wire hazard rate showing a pronounced decreasing-failure regime. (c) Hook reliability (n=16) with narrower uncertainty bounds. (d) Hook hazard rate decreasing more mildly toward the useful-life region. Shaded regions represent 95% bootstrap confidence intervals from 1,000 resamples.



(a)



(b)

Figure 7. Comparative analysis of bootstrap uncertainty propagation and its practical implications for preventive maintenance timing. (a) Normalized reliability curves comparing 95% confidence bands. (b) Maintenance decision framework translating a target reliability threshold R(t) = 0.5 and bootstrap uncertainty into actionable replacement windows.

5. Conclusion

This paper proposes an uncertainty-aware predictive-maintenance workflow that transforms routine maintenance logs into time-between-failures data and estimates component reliability using a location-shifted three-parameter Weibull model. By retaining tied TBF values as separate failure intervals in the median-rank construction, the analysis produces a consistent empirical CDF, Weibull probability plot, and KS goodness-of-fit assessment. Parameter uncertainty is quantified through bootstrap confidence intervals, and model adequacy is checked using both classical and bootstrap-informed KS results.

Applied to two sewing-machine components, the results indicate $\beta < 1$ for both the tension wire and the hook, so both components are governed by decreasing hazard rates and an early-life failure regime. The tension wire shows a strong infant-mortality signature and a wide uncertainty, with a long characteristic life ($\eta = 24$ days) but broad dispersion in failure times. The hook has a short characteristic life ($\eta = 18$ days) and low MTBF, yet its uncertainty bands are narrow; its Weibull fit is acceptable, although the empirical CDF departs visibly from the fitted model around 17 days.

From a maintenance perspective, the analysis supports early post-replacement inspection for both components, strong burn-in and installation control for the tension wire, and focused

time-based replacement planning for the hook. The replacement recommendations are defined explicitly by a reliability-target rule rather than by heuristic judgement: the point intervention age is taken at R(t) = 0.5, and the quoted windows correspond to the ages where the 95% bootstrap reliability bounds cross the same threshold. Under this rule, the hook supports a relatively narrow 12-25 day preventive window, whereas the tension wire requires a broader 10-35 day risk-based decision zone because its uncertainty is much higher. The framework therefore provides a transparent route from sparse maintenance logs to defensible, uncertainty-aware maintenance decisions. Because the sample sizes are limited and the location parameter is sensitive, the recommended windows should be treated as adaptive decision ranges and updated as new failure data become available. while the methods are individually established, the contribution is their integration into a practical, uncertainty-aware workflow for sparse industrial data. Future work should extend the approach to censored or repairable-system data, incorporate operating-condition covariates and condition-monitoring signals, and link the uncertainty-aware reliability outputs to cost-optimised maintenance policies.

Acknowledgement

The author extends her appreciation to the Deanship of Research and Graduate Studies at King Khalid University for funding this work through Large Research Groups Program under grant number RGP2/39/47.

References

1. Heizer J, Render B, Munson C. *Operations management: sustainability and supply chain management*, 14th ed. Harlow: Pearson; 2023.
2. ISO 55000:2024. *Asset management — Vocabulary*. Geneva: ISO; 2024.
3. Siemens AG. *Senseye predictive maintenance. The true cost of downtime 2024: How much do leading manufacturers lose through inefficient maintenance?* Industry report; 2024. https://www.siemens.com; 2024 [accessed 22 February 2026].
4. ISO 13381-1:2025. Condition monitoring and diagnostics of machines — Prognostics — Part 1: General guidelines. Geneva: ISO; 2025.
5. ISO 17359:2018. Condition monitoring and diagnostics of machines — General guidelines. Geneva: ISO; 2018.
6. Zonta T, da Costa CA, Righi RR, de Lima MJ, da Trindade ES, Li GP. Predictive maintenance in Industry 4.0: a systematic literature review. *Computers & Industrial Engineering* 2020; 150: 106889. https://doi.org/10.1016/j.cie.2020.106889.
7. Meeker WQ, Escobar LA, Pascual FG. *Statistical methods for reliability data*, 2nd ed. Hoboken, NJ: Wiley; 2022.
8. Konwerski J, Ziółkowski J, Oszczypała M, Małachowski J, Lęgas A. Analysis of failure data for estimating availability and reliability indicators using statistical and stochastic methods. *Eksploatacja i Niezawodnosc – Maintenance and Reliability* 2026; 28(2): 211577.
9. Selech J, Rogula-Kozłowska W, Piątek P, Walczak A, Pieniak D, Bondaronok P, Marcinkiewicz J. Failure and reliability analysis of heavy firefighting and rescue vehicles: a case study. *Eksploatacja i Niezawodnosc – Maintenance and Reliability* 2024; 26(1): 175505. https://doi.org/10.17531/ein/175505.
10. Genschel U, Meeker WQ. A comparison of maximum likelihood and median-rank regression for Weibull estimation. *Quality Engineering* 2010; 22(4): 236–255. https://doi.org/10.1080/08982112.2010.503447.
11. Zhang Q, Hua C, Xu G. A mixture Weibull proportional hazard model for mechanical system failure prediction utilising lifetime and monitoring data. *Mechanical Systems and Signal Processing* 2014; 43(1–2): 103–112. https://doi.org/10.1016/j.ymssp.2013.10.013.
12. Jiang R, Qi F, Cao Y. Relation between aging intensity function and WPP plot and its application in reliability modelling. *Reliability Engineering & System Safety* 2023; 229: 108894. https://doi.org/10.1016/j.ress.2022.108894.
13. Guo J, Kong X, Wu N, Xie L. Weibull parameter estimation and reliability analysis with small samples based on successive approximation method. *Quality and Reliability Engineering International* 2024; 40(6): 3280–3303.
14. Compare M, Baraldi P, Bani I, Zio E, McDonnell D. Industrial equipment reliability estimation: a Bayesian Weibull regression model with covariate selection. *Reliability Engineering & System Safety* 2020; 200: 106891. https://doi.org/10.1016/j.ress.2020.106891.
15. Zhang CW. Weibull parameter estimation and reliability analysis with zero-failure data from high-quality products. *Reliability Engineering & System Safety* 2021; 207: 107321. https://doi.org/10.1016/j.ress.2020.107321.
16. Zhang F, Shen J, Liao H, Ma Y. Optimal preventive maintenance policy for a system subject to two-phase imperfect inspections. *Reliability Engineering & System Safety* 2021; 205: 107254.https://doi.org/10.1016/j.ress.2020.107254.

17. Safari MAM, Masseran N, Majid MHA, Tajuddin RRM. Robust estimation of the three-parameter Weibull distribution for addressing outliers in reliability analysis. *Scientific Reports* 2025; 15(1): 11516. https://doi.org/10.1038/s41598-025-96043-1.
18. Shangguan A, Feng N, Fei R, Hei X, Jin Y, Mu L. Reliability assessment of competitive failure systems based on three-parameter Weibull distribution and Wiener process. *Eksploatacja i Niezawodnosc – Maintenance and Reliability* 2025; 27(3): 199426. https://doi.org/10.17531/ein/199426.
19. Shangguan A, Feng N, Fei R, Hei X, Jin Y, Mu L. Reliability assessment of competitive failure systems based on three-parameter Weibull distribution and Wiener process. *Eksploatacja i Niezawodnosc – Maintenance and Reliability* 2025; 27(3): 199426. https://doi.org/10.17531/ein/174777.
20. NIST/SEMATECH. Probability plotting (median ranks / plotting positions). In: *NIST/SEMATECH e-Handbook of Statistical Methods*. https://www.itl.nist.gov/div898/handbook/; 2026 [accessed 22 February 2026].
21. Sánchez-Herguedas A, Mena-Nieto A, Rodrigo-Muñoz F. A method for obtaining the preventive maintenance interval in the absence of failure time data. *Eksploatacja i Niezawodnosc – Maintenance and Reliability* 2022; 24(3): 564–573. https://doi.org/10.17531/ein.2022.3.17.
22. NIST/SEMATECH. Weibull plot. In: *NIST/SEMATECH e-Handbook of Statistical Methods*. https://www.itl.nist.gov/div898/handbook/; 2026 [accessed 22 February 2026].
23. Gibbons JD, Chakraborti S. *Nonparametric statistical inference*, 6th ed. Boca Raton, FL: CRC Press; 2021.
24. NIST/SEMATECH. Kolmogorov–Smirnov goodness-of-fit test. In: *NIST/SEMATECH e-Handbook of Statistical Methods*. https://www.itl.nist.gov/div898/handbook/; 2026 [accessed 22 February 2026].
25. Burnham KP, Anderson DR. Model selection and multimodel inference: a practical information-theoretic approach, 2nd ed. New York, NY: Springer; 2002.
26. Barlow RE, Proschan F. *Mathematical theory of reliability*. New York, NY: Wiley; 1965.

Nomenclature

Symbol	Definition	Unit
T	Time / age of component	days
TBF	Time between failures	days
B	Weibull shape parameter (slope)	dimensionless
H	Weibull scale parameter (characteristic life)	days
Γ	Weibull location parameter (failure-free period)	days
F(t)	Cumulative distribution function (unreliability)	dimensionless
R(t)	Reliability function, R(t) = 1 − F(t)	dimensionless
h(t)	Hazard rate (instantaneous failure rate)	failures/day
f(t)	Probability density function	1/days
MTBF	Mean time between failures	days
σ	Standard deviation of time to failure	days
n	Sample size (number of failure intervals)	dimensionless
D_max	Kolmogorov–Smirnov test statistic	dimensionless
D_crit	KS critical value at significance level α	dimensionless
α	Significance level	dimensionless
Γ(·)	Euler gamma function of the second kind	dimensionless
AIC	Akaike Information Criterion	dimensionless
BIC	Bayesian Information Criterion	dimensionless
LL	Log-likelihood	dimensionless
k	Number of model parameters	dimensionless
Cp	Cost of preventive replacement	currency
Cc	Cost of corrective (failure-based) replacement	currency